01 Feb 2001

Gas Holdup in a Trayed Cold-Flow Bubble Column

A. Kemoun

N. Rados

F. Li

M. (Muthanna) H. Al-Dahhan
Missouri University of Science and Technology, aldahhanm@mst.edu

et. al. For a complete list of authors, see https://scholarsmine.mst.edu/che_bioeng_facwork/1362

Recommended Citation

A. Kemoun et al., "Gas Holdup in a Trayed Cold-Flow Bubble Column," *Chemical Engineering Science*, vol. 56, no. 3, pp. 1197 - 1205, Elsevier, Feb 2001.
The definitive version is available at https://doi.org/10.1016/S0009-2509(00)00340-7

PERGAMON

Chemical Engineering Science 56 (2001) 1197–1205

Chemical Engineering Science

www.elsevier.nl/locate/ces

Gas holdup in a trayed cold-flow bubble column

A. Kemoun[a,*], N. Rados[a], F. Li[a], M. H. Al-Dahhan[a], M. P. Dudukovic[a], P. L. Mills[b], T. M. Leib[c], J. J. Lerou[d]

[a]*Chemical Reaction Engineering Laboratory, Department of Chemical Engineering, Washington University, St. Louis, MO 63130-4899, USA*
[b]*Chemical Science and Engineering Laboratory, DuPont Central Research and Development, Experimental Station, E304/A204, Wilmington, DE 19880-0304, USA*
[c]*Reaction Engineering Consultants, DuPont Engineering Technology, 1007 Market Street/N6404, Wilmington, DE 19898-0001, USA*
[d]*DuPont Nylon Intermediates, Sabine River Laboratory, Orange, TX 77630, USA*

Abstract

An experimental study was performed to investigate the effect of sieve trays on the time-averaged gas holdup profiles and the overall gas holdup in a cold-flow bubble column that was scaled-down from a commercial unit. γ-ray computed tomography (CT) was used to scan the column at several axial locations in the presence and absence of trays from which the local variation of the gas holdup was extracted. The overall gas holdup was also determined using the same configuration by comparing the expanded and static liquid heights. Air and water were used as the gas–liquid system. The superficial gas and liquid velocities were selected to span the range of the commercial system using gas spargers having multiple lateral distributors that were also scaled-down from the commercial design. To investigate the impact of sparger hole density on the local and overall gas holdup, two difference sparger designs were used in which the hole density per lateral was varied. The gas hole velocity was maintained constant at ca. 245 m/s, which approached that used in the commercial reactor. It is shown that the local gas holdup determined by CT is generally higher in the tray down comer region and exhibits an asymmetric pattern when trays are present. The use of increased sparger hole density at a constant gas superficial velocity leads to steeper gradient in the gas holdup near the column centerline and a higher overall gas holdup. These findings suggest that the performance of bubble column reactors for various applications is sensitive to both sparger and tray design.

Keywords: Bubble column; Multiphase; Internals; Holdup; Tomography; Trays; Profiles; Spargers

1. Introduction

Stage-wise mass transfer operations, such as distillation, extraction, absorption, leaching, ion exchange, and drying, to name a few, typically utilize processing equipment with internals to promote intimate contacting between the various phases so that phase equilibrium can be approached for a given stage (cf., King, 1971; Sherwood, Pigford & Wilke, 1975). When mass transfer is accompanied by chemical reaction in a multiphase contactor, the incorporation of internals is generally known to reduce the overall back mixing of each phase so that the benefits of reactor operation as an ideal cascade can be approached (Westerterp, van Swaaij & Beenackers, 1987). Besides modifying the microscale and macroscale flow patterns of the various phases, the addition of internals could alter various hydrodynamic and transport parameters that can potentially impact reactor performance, such as fluid holdups, multiphase flow pressure drop, phase voidage distributions, local fluid mixing, interphase mass transfer coefficients, and interfacial areas.

The ability to either scale-up new multiphase reactors, or to analyze the performance of existing ones, is clearly dependent upon understanding and quantifying local transport–kinetic interactions, flow and contacting patterns of the various phases, and how these change with operating conditions (Dudukovic', Larachi & Mills, 1999). For certain types of more common internals, such as trays and packing, used in staged mass transfer contactors, a significant body of literature exists on scale-up guidelines and methods for estimating hydrodynamic and transport parameters using empirical correlations (cf., Fair, 1985; Sloley, 1999). Information on the selection

* Corresponding author.

0009-2509/01/$ - see front matter
PII: S0009-2509(00)00340-7

and performance of internals in gas–liquid catalytic reactors, such as trickle-beds, bubble columns, and ebullated beds, is very limited in the open literature. For example, the use of perforated trays to reduce liquid-phase back mixing in bubble columns has been summarized by Deckwer (1992), while gas holdup and pressure drop data from two different tray designs has also been reported (Chen, 1986). Most of the information on internals is usually confined to either patent teachings (cf., Nutter, 1995; Resetarits, 1992), or is maintained as company proprietary knowledge for a specific process. Hence, experimental data on such devices would be useful in certain multiphase reactor applications, as their performance is needed for rational selection and design purposes. With the continuing evolution of advanced fluid dynamic simulations of multiphase systems (Dudukovic' et al., 1999; Kuipers & van Swaaij, 1997), and invention of non-invasive experimental methods for monitoring of multiphase flows (Chaouki, Larachi & Dudukovic', 1997), the development of improved constitutive relationships for more accurate fluid dynamical predictions in complex geometries will continue to evolve. Hence, a priori prediction of how various internals affect the multiphase fluid dynamics in the absence of chemical reaction should eventually become more reliable. Experimental data that can be used for guiding the design and scale-up of reactors with the current state-of-the-art approaches is still required, however.

The primary objective of this work is to perform an experimental study on the hydrodynamics of a cold-flow bubble column reactor with trays that was scaled-down from a commercial unit, and to compare the results to those obtained for the empty reactor, i.e., to the identical unit without any trays. Particular emphasis is placed upon the effect of the sparger design (hole density) and the trays on the local gas holdup profiles as measured by γ-ray computed tomography (Kumar, Moslemian & Dudukovic', 1995) and overall gas holdup as determined by the fast shutoff of the gas and liquid lines.

2. Cold-flow unit experimental system

The cold-flow system is equipped with a column along with various sub-systems for feeding and controlling the volumetric flow rates of air and water. The liquid delivery system was connected to a centrifugal pump and the rotameter to control the liquid flow rate. The liquid was introduced to the top of the column through a shower-type distributor that was located about 13.9 cm above the top tray (Fig. 1). The liquid exited the column bottom through a plenum, and then flowed into a surge tank. A second centrifugal pump was used to recycle the liquid back to the main feed tank. The air was supplied from the house supply system, which had a delivery pressure of about 841 kPa. After flowing through a filter, it was introduced to a rotameter and then connected to the sparger.

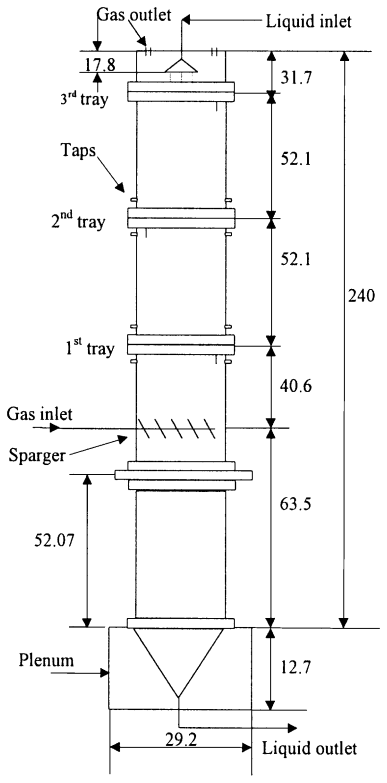

Fig. 1. Schematic diagram of the column used for the cold-flow studies (all dimensions are given in cm).

A schematic of the cold-flow column design is provided in Fig. 1. It was constructed of clear acrylic tubing, and had a nominal diameter of 0.2 m and an overall height of 2.4 m. The column was divided into four sections where each section had an overall height of 0.52 m. Three sieve trays were located between each section. The top and bottom trays were used to account for entrance and exit effects.

Several ports were installed in the middle stage and also across the trays so that pressure transducers and liquid conductivity probes could be inserted for local measurement of the pressure fluctuations and liquid-phase tracer concentrations. Another identical column without these ports was also constructed and used for the γ-ray computed tomography (CT) measurements. The ports were omitted to reduce the interference of the nuclear radiation that might otherwise occur during collection of the tomographic data.

A schematic of the tray design and hole layout is shown in Fig. 2. The trays were constructed of 6.35 mm thick acrylic sheet and contained 42 holes having a diameter of 6.35 mm each that were laid out on a triangular pitch. The down comer occupied about 10% of the total tray cross-sectional area. The latter was a copy of the one

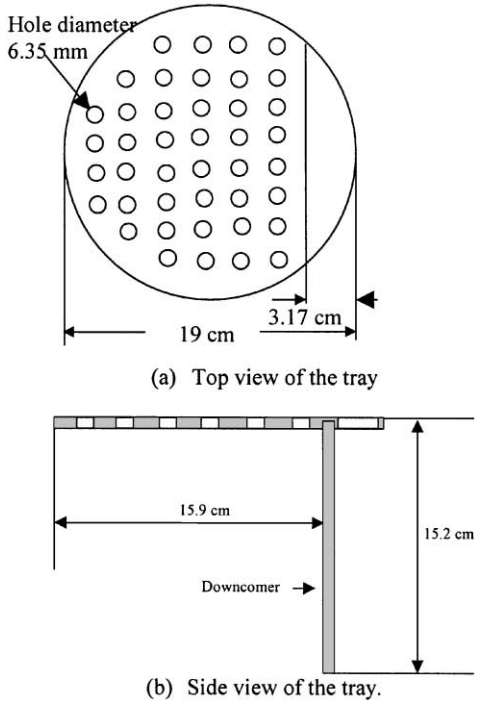

Fig. 2. Schematic of the tray design.

used in the commercial system, which was mounted flush with the top of the tray.

The dimensions for the column diameter, tray spacing, tray geometry, and tray hole diameter were determined by applying scaling principles to a commercial-scale system. The key concepts that were used included equality of gas and liquid mass velocities, hydrodynamic head, tray hole velocity and pressure drop, and phase residence times on a stage. The details are omitted for brevity but appeared to provide a reasonable first basis for scale-down of the commercial system.

The spargers in the cold-flow unit were scaled down using operating conditions and mechanical data were extracted from the commercial-scale sparger design. To obtain gas mass velocities in the cold-flow unit that were in the same range as those used on a given tray in the commercial system, a gas jet velocity of ca. 180–245 m/s from each respective sparger hole was required.

Details on the sparger design are shown in Fig. 3. Ten laterals were welded to the main gas distribution manifold with the lateral lengths being selected so the sparger fits into the column with a clearance of 6–12 mm. As shown in Fig. 4, each lateral was drilled with either 40 or 200 holes with a hole diameter of 350 μm. The total number of holes in a lateral was varied to maintain nearly the same gas hole velocity as the gas volumetric flow rates were varied from 0.944,2.36, and 4.72 l/s at STP. The holes were drilled to give an offset angle of 30° from the vertical and were arranged so that they pointed

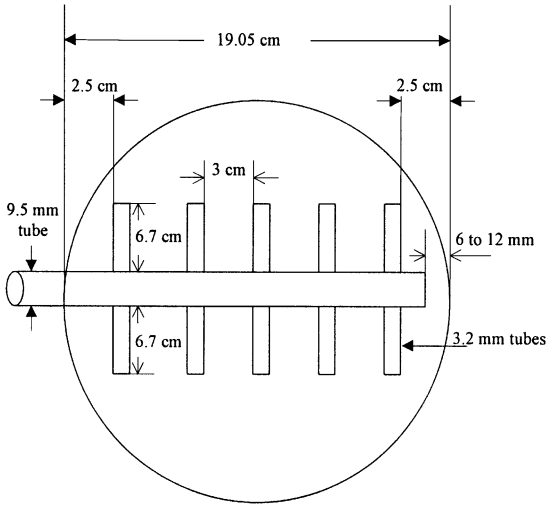

Fig. 3. Design of the gas sparger.

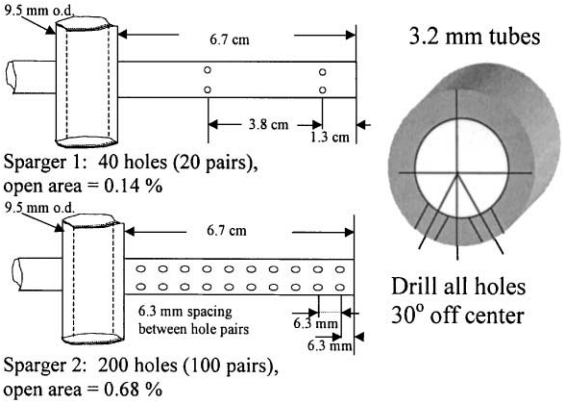

Fig. 4. Details on the hole schedule for the gas sparger laterals.

Table 1
Range of operating conditions

Liquid flow rate (l/s)	0.13–0.41
Gas flow rate (l/s)	1.98–4.75
Gas velocity through the sparger holes: sparger #1	$U_h \cong 245.24$ m/s at superficial gas velocity $U_g = 3.33$ cm/s
Gas velocity through the sparger holes: sparger #2	$U_h \cong 245.24$ m/s at $U_g = 16.65$ cm/s
Gas and liquid phases	Air and water
Liquid superficial velocity U_l(cm/s)	0.4–1.42
Gas superficial velocity U_g (cm/s)	1.6–16.7

downward. The sparger assembly was mounted 0.41 m below the first tray from the bottom of the column. The gas was introduced to the main sparger supply line through a 9.5 mm o.d. manifold.

The operating conditions, which were scaled down from the commercial reactor system, used in this study are summarized in Table 1.

3. γ-ray computed tomography

Computed tomography (CT) was used to determine the time-averaged cross-sectional variation of the gas holdup at various axial column locations. The particular axial positions where CT scans were made are shown in Fig. 5. These were selected to provide gas holdup profiles both above and below the first tray, below the second tray, and halfway between the first and second trays. To assess the effect of sparger hole density on the gas holdup profile, the CT scans were performed at levels 2–4 using the sparger having the lowest hole density (sparger no. 1, Fig. 4), at a superficial gas velocity of 3.33 cm/s and superficial liquid velocity of 0.44 and 0.88 cm/s, respectively. The CT scans were then repeated at all axial locations shown in Fig. 5 using the sparger having the greatest hole density (sparger no. 2, Fig. 4) at $U_g = 16.65$ cm/s and $U_l = 0.44$ and 1.1 cm/s, respectively. To assess the effect of the trays on the local gas holdup profiles, the trays were removed and the scans were repeated at the latter set of conditions as well as $U_l = 0$ cm/s corresponding to a batch liquid.

The scanner used here is based upon a third-generation fan-beam configuration developed at Washington University. Details of the hardware and software have been described in previous work (Kumar et al., 1995; Kumar, Dudukovic' & Toseland, 1997). The scanner design consists of an array of NaI (TI) detectors with a diameter of 5 cm as well as an encapsulated 92 mCi ^{137}Cs source located opposite to the center of the array of detectors. Five detectors were used for the present study, which can cover the whole cross section of the column. The detectors and the source are mounted on a plate, which can be rotated around the axis of the column by a stepping motor that is controlled through a microprocessor. Moreover, the whole assembly can be moved in the axial direction along the column to scan different axial levels of the column. This design of the CT scanner yields a spatial resolution of ca. 0.35 cm in the horizontal direction and 1.0 cm in the vertical direction.

The tomographic attenuations were measured along a number of beam paths through the column from different coordinates. Once a set of attenuation measurements was completed, the density distribution image was reconstructed by using a suitable reconstruction algorithm. In this work, the estimation–maximization (Kumar, 1994) was used since it has the following advantages: (1) it accounts for statistical variations associated with radiation measurements; (2) it readily incorporates non-uniform beam effects; and (3) it ensures that the final reconstruction will contain positive values. To obtain statistically significant results, and to reduce the effect of position, the CT scans were conducted around the column using a total scanning time of 2 h.

4. Results and discussion

Both the local and overall gas holdups obtained in the presence and absence of the trays as determined by CT and the simultaneous shutoff of the gas and liquid lines technique are compared in this section for the two different types of sparger designs.

4.1. Computed tomography results

Fig. 6a shows that the gas holdup distribution at level 2, which is 7.62 cm above the first tray, is asymmetric. Fig. 6b shows that when the superficial liquid velocity is increased to 1.1 cm/s, the asymmetry is more pronounced. The region of high gas holdup contours show that the maximum gas holdup at level 2 is ca. 11% at $U_l = 0.44$ cm/s (Fig. 6a) and ca. 10.5% at $U_l = 1.1$ cm/s (Fig. 6b).

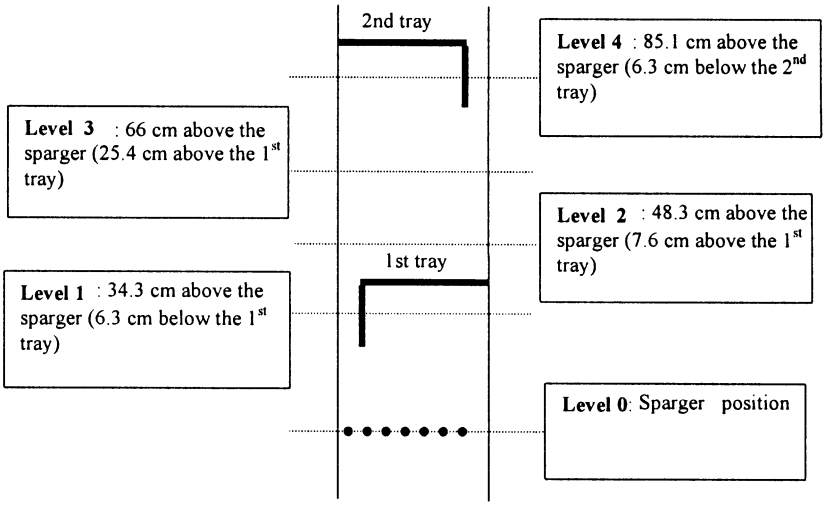

Fig. 5. Axial positions of the CT scans.

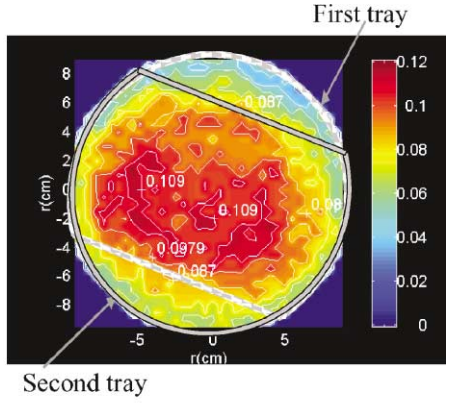

(a) U_g=3.3 cm/s and U_l=0.44 cm/s.

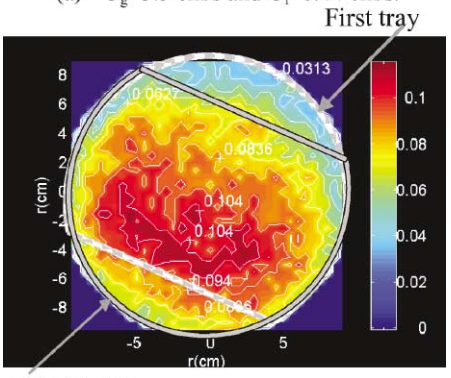

(b) U_g=3.3 cm/s and U_l=1.1 cm/s.

Fig. 6. Gas holdup distribution for sparger no. 1 at level 2.

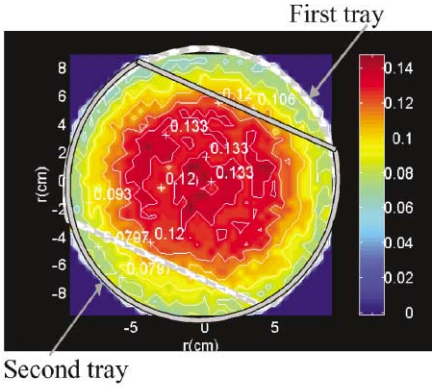

(a) U_g=3.3 cm/s and U_l=0.44 cm/s.

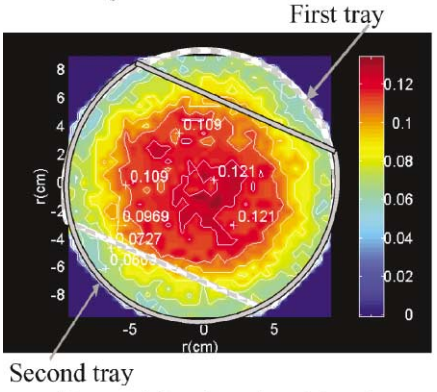

(b) U_g=3.3 cm/s and U_l=1.1 cm/s.

Fig. 7. Gas holdup distribution for sparger no. 1 at level 3.

Fig. 7a is similar in concept to Fig. 6a, except it shows the gas holdup distribution at level 3, which is 25.4 cm above the first tray. The gas holdup distribution between the trays is now symmetric at both superficial liquid velocity of 0.44 and 1.1 cm/s, respectively. This differs from the results in Fig. 6a corresponding to level 2 (7.6 cm above the first tray), where the gas holdup distribution was asymmetric at the same liquid from rates. Inspection of the gas holdup distribution contours shows that the maximum gas holdup decreases from 13.3% at $U_l = 0.44$ cm/s (Fig. 7a) to 12.1% at $U_l = 1.1$ cm/s (Fig. 7b).

Fig. 8 shows the gas holdup distribution at level 4, which is 6.35 cm below the second tray. A region of reduced gas holdup occurs in the tray down comer region. The regions of higher gas holdup are positioned in the center of the column for $U_l = 0.44$ cm/s. This region of increased gas holdup moves further from the down comer when the superficial liquid velocity is increased from 0.44 to 1.1 cm/s.

The experiments described above, which correspond to the sparger having a low hole density, were repeated using the sparger having the highest hole density. The same superficial liquid velocities were used (0.44 and 1.1 cm/s, respectively), but the superficial gas velocity was increased from 3.3 and 6.6 to 16.6 cm/s so that the same gas jet velocity was maintained through the sparger holes. A comparison between the gas holdup profiles for the two different spargers shows that at level 1, which is just 6.35 cm below the first tray, the highest gas holdup occurs in the center of the column at both liquid flow rates. The holdup is relatively insensitive as the superficial liquid velocity is increased from 0.44 to 1.1 cm/s at $U_g = 16.6$ cm/s, which is the highest rate used. The same behavior is also noted at level 2, which is 7.62 cm above the first tray, except a region of lower gas holdup occurs closest to the column wall.

The symmetry of the cross-sectional gas holdup at level 3 allows the azimuthally time-averaged radial gas holdup profiles to be determined. The results are compared in Fig. 9 at various gas and liquid flow rates. At the highest superficial gas velocity ($U_g = 6.7$ cm/s), the gas holdup profile increases as the superficial liquid velocity is increased from $U_l = 0.44$ to 1.1 cm/s. At the lowest superficial gas velocity used ($U_g = 3.3$ cm/s), the opposite behavior occurs, i.e., the gas holdup profile decreases when the liquid flow rate increases. At level 3 which is halfway between the two trays, and level 4, which lightly below the second tray, the gas holdup is relatively insensitive to variations in liquid flow rate. The region of

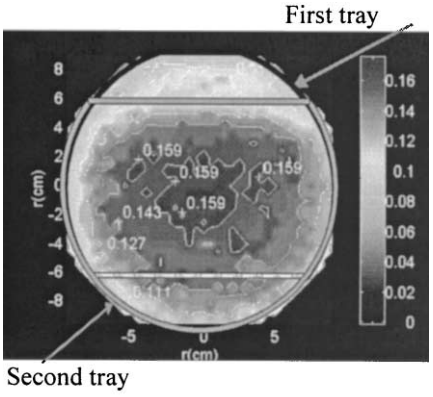

(a) U_g=3.3 cm/s and U_l=0.44 cm/s.

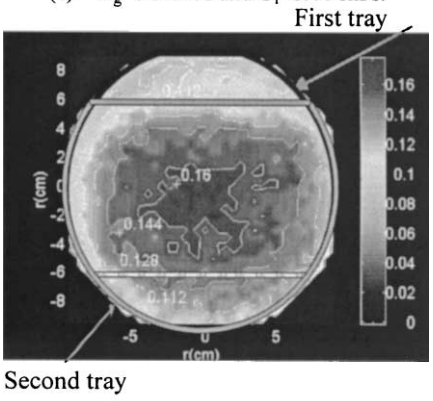

(b) U_g=3.3 cm/s and U_l=1.1cm/s.

Fig. 8. Gas holdup distribution for sparger no. 1 at level 4.

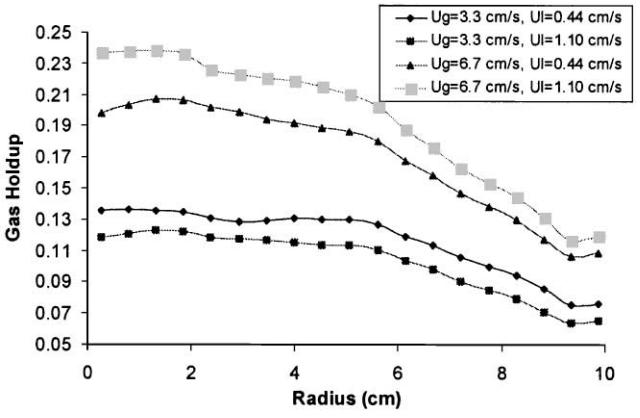

Fig. 9. Azimuthally time-averaged radial gas holdup at the middle of the stage obtained with sparger no. 1.

the lowest gas holdup is in the down corner or slightly below it.

CT scans were also conducted by removing the trays to create an open column interior. The superficial liquid velocities used were 0 (batch liquid), 0.44 and 1.1 cm/s, while the superficial gas velocity was set at $U_g = 16.6$ cm/s. The scanner was positioned halfway between the first and second trays, which corresponds to level 3 in Fig. 5.

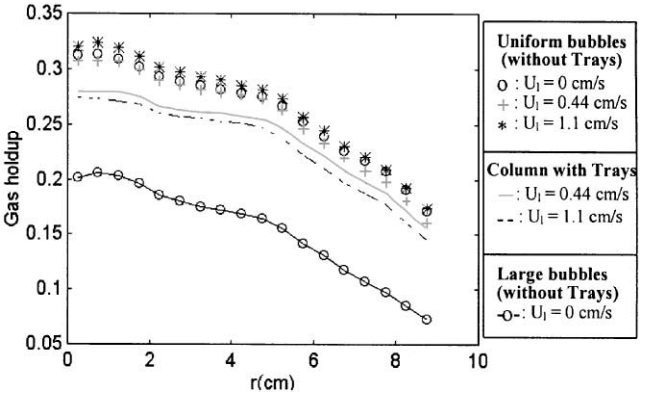

Fig. 10. Comparison of the gas holdup profiles at a superficial gas velocity $U_g = 16.6$ cm/s at various liquid flow rates in a column with and without trays.

A comparison between the gas holdup profiles obtained in the presence and absence of trays is given in Fig. 10. The CT data for the situation where trays were removed was first processed to evaluate the azimuthally time-averaged radial gas holdup associated with uniform bubbles whose diameters were visually estimated to be about 5–10 mm (upper set of data points). Next, the azimuthally time-averaged radial gas holdup was also determined for the experiment associated with the large bubbles of 30–50 mm bubble sizes that mainly exist in the center of the column (lowest set of data points). This difference in these two experiments was the result of different surface tension due to the impurity of the water, which infected the system as for example one-drop of oil can generate formation of large bubbles. These large bubbles rise quickly and lead to a decreased gas holdup. The gas holdup profiles obtained for the column with trays is seen to fall between the gas holdup of the uniform bubbles and large bubbles. The highest gas holdup for this case is obtained at the lowest superficial liquid velocity used (0.44 cm/s). The presence of both the uniform and large bubbles in the empty column suggests that two different hydrodynamic regimes exist in the same column due to the purity of the water.

Fig. 10 also shows that the gas holdup profiles obtained in the empty column without trays are only slightly affected by the liquid flow rate over the range of superficial liquid velocities (0, 0.44 and 1.1 cm/s) that were studied. The gas holdup profiles for the empty column have a larger gradient than those obtained in the column with trays. This finding suggests that one function of the trays is to create an obstacle for the uniform bubbles, and to induce bubble coalescence to produce some large bubbles. These larger bubbles eventually escape the stage through the down comer and are captured by the second tray. The flow visualization also reveals the appearance of large bubbles that are about 20–30 mm in diameter in the trayed column. The CT scans also

confirm that a high concentration of gas exists below the trays, which seems to induce bubble coalescence.

4.2. Overall gas holdup

The combined effects of the sparger hole density, gas flow rate, liquid flow rate, and presence or absence of sieve trays on the overall gas holdup were determined using the simultaneous shut-off of the air, input and output water lines. The difference between the expanded height (before the shut-off) and the static height (after the shut-off) leads to the overall gas holdup.

It is well accepted that gas sparger design and performance can have a significant effect on both the local and overall gas holdups in bubble column reactors. Use of fundamental mass and momentum conservation principles to provide detailed a priori predictions of performance for typical commercial-scale spargers using computational fluid dynamics is not possible using existing knowledge. This is mainly due to the existence of a large number of sparger holes that are typically present in commercial-scale gas-sparger designs, and difficulties associated with modeling high velocity, multiple interacting gas jets into a gas–liquid dispersion. Another complicating feature is that the gas-sparger performance is also dependent on the column aspect ratio as well as the liquid physical properties, both of which influence coalescence and breakup of the gas bubbles (Kumar, 1994).

The sparger designs used here were identical except for the total number of sparger holes, which translates into a difference in the hole density or the number of holes per unit column cross-sectional area. The total number of holes per lateral and hole diameter was selected so that the same gas velocity through the holes could be obtained when the superficial gas velocity changed from $U_g = 3.3$ to 16.6 cm/s. This particular range for the superficial gas velocity produced a gas velocity that approached the commercial system, namely, $U_h = 245$ m/s.

Fig. 11 compares the effect of the number of sparger holes on the overall gas holdup as a function of the gas flow rate at a constant liquid volumetric flow rate. The sparger with the greatest number of holes per unit column cross-sectional area (sparger no. 2) always provides a larger overall gas holdup over the indicated range of gas and liquid volumetric flow rates. The same trend in the gas holdup was observed at other liquid flow rates. For a given sparger, the gas velocity through the sparger holes was variable owing to the use of variable gas volumetric flow rates.

The results for sparger having the lowest density of holes are shown in Fig. 12. When the superficial gas velocity exceeds $U_g = 4.2$ cm/s, the overall gas holdup increases when the superficial liquid velocity is increased from $U_l = 0.44$ to 1.1 cm/s for a fixed value of the superficial gas velocity. However, when the superficial liquid

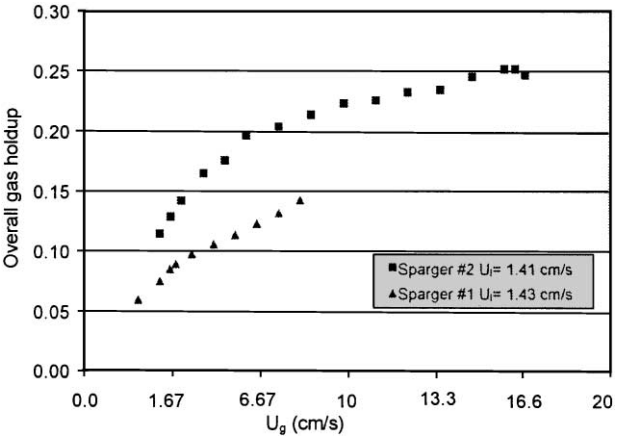

Fig. 11. The effect of sparger no. 2 hole density on the overall gas holdup.

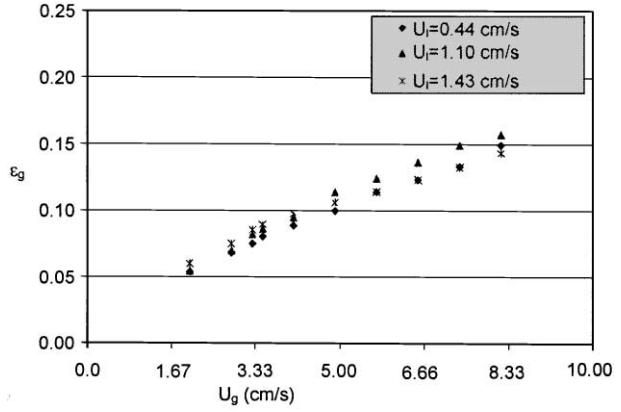

Fig. 12. Overall gas holdup using the sparger no. 1.

velocity is increased further from $U_l = 1.1$ to 1.43 cm/s, the overall gas holdup undergoes a reduction for a fixed value of the superficial gas velocity. This behavior could be due to the formation of larger bubbles by coalescence of smaller bubbles. It should also be noted that when the sparger is operated at a superficial gas velocity of 3.3 cm/s, the gas velocity through the sparger holes is nearly the same as that used in the commercial unit ($U_h = 245$ m/s).

The overall gas holdup data obtained using the sparger having the greatest density of holes per unit cross-sectional area of the column are illustrated in Fig. 13. When superficial gas velocities exceed 4.16 cm/s, the overall gas holdup decreases as the superficial liquid velocity is increased from 0.44 to 0.77 cm/s, and from 1.1 to 1.41 cm/s. However, at a superficial gas velocity of $U_g = 16.65$ cm/s, which translates into a gas hole velocity for the commercial unit ($U_h = 245$ m/s) for this particular sparger hole density, the overall gas holdup slightly increases when superficial liquid velocity is increased from 0.44 to 0.77 cm/s. The overall gas holdup then

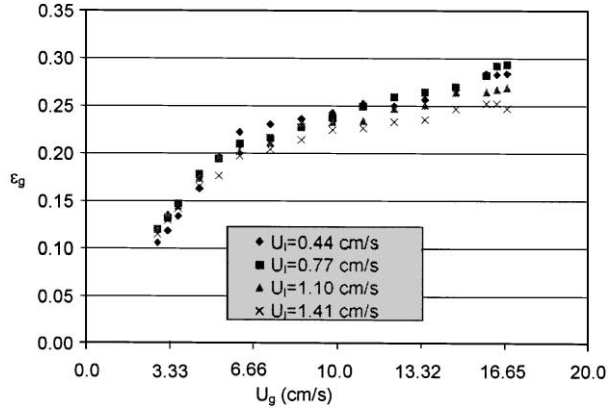

Fig. 13. Overall gas holdup using the sparger no. 2.

decreases slightly when the superficial liquid velocity is increased further to 1.41 cm/s.

The CT-based results for the time-averaged cross-sectional gas holdup profiles that were obtained between trays 1 and 2 (middle of the stage) with sparger no. 1 show that when $U_g < 5$ cm/s, the gas holdup decreases slightly when the superficial liquid velocity is increased from 0.44 to 1.10 cm/s. However, when $U_g > 5$ cm/s, the gas holdup increases when the superficial liquid velocity is increased from 0.44 to 1.10 cm/s. This agrees with the trend for the overall gas holdup that is illustrated in Fig. 12, which provides some partial confirmation between the two independent experimental methods.

The effect of column internals on the overall gas holdup was also investigated by removing the trays and repeating the measurements using identical values for the superficial gas and liquid velocities. It was found that the overall gas holdups were nearly the same, even though the axial and radial profiles were not. For the geometry and conditions studied in this work, this appears to contradict arguments suggesting that the trays reduce bubble coalescence and produce higher overall gas holdups.

5. Summary and conclusions

An experimental system was developed to study the local and overall gas holdup in a trayed bubble column reactor under cold-flow conditions. Many commercial bubble column reactors employ trays and other types of internals to control gas–liquid contacting, but limited design information is available.

The gas holdup profiles were determined using γ-ray computed tomography. Measurements were made at different axial locations using two different gas spargers. The gas holdup profiles are generally affected by the superficial velocities of the gas and liquid, the gas sparger geometry, and the presence or absence of the trays. The gas holdup distribution can be either symmetric or asymmetric depending upon various hardware and operational variables. The gas holdup generally decreases from the column center toward the column wall, and the region of higher gas holdup can shift toward the wall with an increase in the superficial velocity of the liquid. The effect of the number of sparger holes per lateral on the gas holdup cannot be neglected and needs to be carefully considered for a given set of process conditions.

The gas holdup profile in bubble column reactors is affected by the presence of internal trays that provide a staging effect, as well as by the sparger design. The use of available engineering correlations for prediction of gas holdup can lead to incorrect estimates since they are based on empty bubble columns without any internals.

The overall gas holdup was also measured using spargers having a different hole density over a range of gas and liquid superficial velocities. The holdup was relatively unaffected by the liquid superficial velocity for the range studied ($0.46 \leqslant U_l$ (cm/s) < 1.52 cm/s), but it increased with increasing gas superficial velocity. The effect of column internals on the overall gas holdup was also investigated by removing the trays and repeating the measurements using identical values for the superficial gas and liquid velocities. It was found that the overall gas holdups were nearly the same, even though the axial and radial profiles were not. For the geometry and conditions studied in this work, this appears to contradict arguments suggesting that the trays reduce bubble coalescence and produce higher overall gas holdups.

References

Chaouki, J., Larachi, F., & Dudukovic', M. P. (Eds.) (1997). *Non-invasive monitoring of multiphase flow* Amsterdam: Elsevier.

Chen, B. H. (1986). Axial dispersion and heat transfer in gas–liquid bubble columns. In N. P. Cheremisinoff (Ed.), *Handbook of heat and mass transfer*. Vol. 2: Mass transfer and reactor design (pp. 1005–1028). Houston: Gulf Publishing.

Deckwer, W. D. (1992). *Bubble column reactors*. New York: Wiley.

Dudukovic', M. P., Larachi, F., & Mills, P. L. (1999). Multiphase reactors — revisited. *Chemical Engineering Science*, *54*, 1975–1995.

Fair, J. R. (1985). Stagewise mass transfer processes. In A. Bisio, & R. L. Kabel (Eds.), *Scaleup of chemical processes* (pp. 431–503). New York: Wiley-Interscience.

King, C. J. (1971). *Separation processes* (pp. 146–211). New York: McGraw-Hill.

Kuipers, J. A. M., & van Swaaij, W. P. M. (1997). Application of computational fluid dynamics to chemical reaction engineering. *Reviews in Chemical Engineering*, *3*, 1.

Kumar, S. B. (1994). Computer tomographic measurements of void fraction and modeling of the flow in bubble columns. *Ph.D. Thesis,* Florida Atlanta University, Boca Raton, FL.

Kumar, S. B., Moslemian, D., & Duduckovic', M. P. (1995). A gamma-ray tomographic scanner for imaging void fraction distribution in bubble columns. *Flow Measurement Instruments*, *6*, 61.

Kumar, S. B., Duduckovic', M. P., & Toseland, B. A. (1997). Measurement techniques for local and global fluid dynamic quantities in two and three-phase systems. In J. Chaouki, F. Larachi, & M. P. Dudukovic' (Eds.), *Non-invasive monitoring of multiphase flows* (pp. 1–46). Amsterdam: Elsevier.

Nutter, D. E. (1995). Gas–liquid contacting apparatus including trays with vapor apertures in overlapping panel margins. *US Patent* 5,468,425, November 21.

Resetarits, M. R. (1992). Multiple down comer contacting tray with fluid-directing baffles. *US Patent* 5,098,615, March 24.

Sherwood, T. K., Pigford, R. L., & Wilke, C. R. (1975). *Mass transfer* (pp. 593–666). New York: McGraw-Hill.

Sloley, A. W. (1999). Should you switch to high capacity trays? *Chemical Engineering Progress,* 94, 23–35.

Westerterp, K. R., van Swaaij, W. P. M., & Beenackers, A. A. C. M. (1987). *Chemical reactor design and operation* (pp. 160–226). Chicester: Wiley.